

Profile characteristics of temporal stability of soil water storage in two land uses

She Dongli · Liu Dongdong · Liu Yingying · Liu Yi ·
Xu Cuilan · Qu Xin · Chen Fang

Received: 10 October 2012 / Accepted: 11 January 2013 / Published online: 24 January 2013
© Saudi Society for Geosciences 2013

Abstract Information on soil water storage (SWS) within soil profiles is essential in order to characterize hydrological and biological processes. One of the challenges is to develop low cost and efficient sampling strategies for area estimation of profile SWS. To test the existence of certain sample locations which consistently represent mean behavior irrespective of soil profile wetness, temporal stability of SWS in ten soil layers from 0 to 400 cm was analyzed in two land uses (grassland and shrub land), on the Chinese Loess Plateau. Temporal stability analyses were conducted using two methods viz. Spearman rank correlation coefficient (r_s) and mean relative differences. The results showed that both spatial variability and time stability of SWS increased with increasing soil depth, and this trend was mainly observed at above 200 cm depth. High r_s ($p < 0.01$) indicated a strong temporal stability of spatial patterns for all soil layers. Temporal stability increased with increasing soil depth, based on either r_s or standard deviation of relative difference index. The boundary between the temporal unstable and stable layer of SWS for shrub land and grassland uses was 280 and 160 cm depth, respectively. No single location could represent the mean SWS for all ten soil layers. For temporal stable layers, however, some sampling locations

could represent the mean SWS at different layers. With increasing soil depth, more locations were able to estimate the mean SWS of the area, and the accuracy of prediction for the representative locations also increased.

Keywords Temporal stability · Soil water storage · Land use · Soil depth

Introduction

Soil water storage (SWS) is an important soil quality indicator as it plays a key role in a series of hydrological and biological processes. In shallow soil layers, SWS has crucial effects on surface and subsurface runoff generation, erosion, plant growth, and material exchange of land-atmosphere system. On the other hand, SWS of deep layers along the soil profile has long been recognized as a water buffering pool for alleviating the effect of drought on plant growth and on the flux of moisture returning to the atmosphere, especially in semi-arid environments. Therefore, the evaluation of characteristics and dynamics of deep profile SWS is helpful for hydrological modeling, improving water resource management practices and vegetation restoration strategy.

Profile SWS is a result of equilibrium between infiltration and evapotranspiration. For the loessal soil profile in China, soil water recharge can reach 120 cm deep on monthly and seasonal scales (She et al. 2010). Indigenous flora extract the water stored in the diverse soil layers, resultantly SWS is highly variable due to soil variability and root distribution. Spatio-temporal variability of SWS has been studied extensively in the past half century (Qiu et al. 2001; Ibrahim and Huggins 2011). The variability of SWS necessitates the collection of numerous samples to acquire a complete picture of its spatio-temporal pattern, which is costly in time

S. Dongli · L. Dongdong · L. Yingying
Key Laboratory of Efficient Irrigation-Drainage and Agricultural
Soil-Water Environment in Southern China, Ministry of Educa-
tion, College of Water Conservancy and Hydropower Engineering,
Hohai University, Nanjing 210098, China

S. Dongli · L. Yi · C. Fang (✉)
Key Laboratory of Aquatic Botany and Watershed Ecology,
Wuhan Botanical Garden, Chinese Academy of Sciences,
Wuhan 430074, China
e-mail: fchenipni@126.com

X. Cuilan · Q. Xin
Jiangsu Provincial center for Land Consolidation and Rehabilitation,
Nanjing, Jiangsu 210024, China

and money. Actually, for most practical applications, the information about mean SWS values and variances are generally sufficient (Tallon and Si 2004). Traditional sampling methods assume that spatial patterns of variability in soil water are random. However, factors controlling soil water exhibit non-random patterns that may persist over time. Therefore, development of new methodologies for the optimized and efficient SWS measurements without losing information is of the utmost importance (Hu et al. 2010a).

The temporal stability concept introduced by Vachaud et al. (1985) has been widely applied as a tool to optimize the sampling scheme. Temporal stability can be described as the capacity of certain locations conserving the property to represent mean and extreme values of the field water content over time (Vachaud et al. 1985; Martínez-Fernández and Ceballos 2003). Based on this concept, it is possible to find locations that represent an area's mean moisture content, to up- and down- scale soil moisture measurements, to complete dataset with missing data and to assimilate data in hydrological modeling (Vanderlinden et al. 2012; Penna et al. 2013). Thus, the concept of temporal stability has been gradually enriched and developed over different areas worldwide, especially during the soil moisture sampling campaigns aimed at the validation of remotely sensed mean soil moisture estimation as summarized in Table 1 (Starks et al. 2006; Cosh et al. 2008; Hu et al. 2010b). With the aim of identifying locations of temporal stability of soil moisture, numerous scientists have mainly investigated the statistical properties of soil moisture in the time domain, and then, described the effects of soil properties and topography, vegetation and land use change, soil depth and monitoring frequency on the stability of water moisture patterns (Martínez-Fernández and Ceballos 2003; Thierfelder et al. 2003; Grant et al. 2004; Brocca et al. 2009; Williams et al. 2009; Hu et al. 2010a; She et al. 2012). A general feature of these previous studies was that (1) few efforts refer to the whole soil profile; (2) even fewer studies examine the temporal stability of soil moisture as a function of depth; (3) some only observe the soil profile within 0–1 m layer. If a subset of the sampling locations could be used to represent the averages of SWS for an area of interest at various levels in the soil profile, as well as the total profile, the temporal stability analysis could reduce the number of field sampling sites required for accurately characterizing the behavior of profile SWS of the study area over time. Very few reports referred to the profile characteristics of SWS temporal stability deeper than 1 m (Hu et al. 2010b; Gao and Shao 2012a). Through the analysis of temporal stability of SWS in 0–1, 1–2, and 2–3 m soil layers using Spearman rank correlation coefficients and relative differences, Gao and Shao (2012a) concluded that the temporal stability of SWS is soil depth dependent which requires more research to be confirmed. Heathman et al. (2009) analyzed the temporal

stability of surface and profile moisture at the field and watershed scales in the Little Washita River Watershed. They suggested that the actual scale of observation and number of measurements affects the relationship between surface and average profile soil moisture temporal stability analysis. Considering the dependence of temporal stability on depth, caution should be taken in devising a sampling plan to determine SWS values for the different soil depths.

Besides the uncertain effects of soil depth on SWS temporal stability, no consistent conclusions have been drawn on the importance of contributing factors to temporal stability. da Sivaró et al. (2001) and Hu et al. (2009) found that soil particle size and organic matter content were the main factors influencing temporal stability. In contrast, Schneider et al. (2008) found that soil characteristics could not fully explain the quality of temporally stable locations. Other studies found that topography and land use rather than soil properties appeared to be the primary factors (Gómez-Plaza et al. 2000; She et al. 2012). Grayson and Western (1998) and Vivoni et al. (2008) believed that the best locations to represent the mean soil water content of a catchment should be the locations which capture the average characteristics of that catchment, e.g., near- to mid-slopes or mid aspects (Grayson and Western 1998). Tallon and Si (2004) found little correlation between temporally stable locations and any of the standard local (soil texture) or non-local (elevation, catchment area, wetness index, and slope curvature) factors that typically affect soil moisture. Nevertheless, the interactive effects of multi-factors, such as land use and soil depth, on identifying representative locations warrants further research.

The Loess Plateau is famous in the world for its deep loess, intense soil erosion, and “Grain-for-Green” re-vegetation programs. Studies on the temporal stability of soil properties on the Loess Plateau of China have gained interest since the recent work by Hu et al. (2009). With more slope farmlands converted to grassland/forestland by planting perennial plants, the profile characteristics and dynamics of SWS become more complex, mainly due to modifications in infiltration rate, runoff intensity, and evapotranspiration. Thus, land use can serve as a good criterion for locating soil moisture measurement locations for catchment mean estimation (She et al. 2012). Since land use and soil depth are two of the main factors controlling soil moisture variability in the Loess Plateau (Hu et al. 2010b), the study of profile characteristics of temporal stability of SWS under various land use systems can be very important, especially for soil water management during the process of vegetation restoration.

The purpose of this present study was to investigate the temporal stability of SWS for ten soil layers down to 400 cm depth in two land uses within a watershed on the Loess Plateau of China. Specific objectives were (1) to determine

Table 1 Main characteristics of the soil moisture temporal stability analysis reported in scientific literature

Research	Study area	Land use	Soil type	Area/length	Sample depth(cm)	Number of sampling points	Number of sampling campaigns
Vachaud et al. (1985)	Grenoble France	Grass	Silty clay sand	2E+03 m ²	100	17	24
	Sevilla Spain	Agric.	/	/	100	9	8
	Moma Tunisia	/	Silty clay sand	100 m	100	19	2
Kachanoski and De Jong(1988)	Saskatchewan Canada	/	/	720 m	10-170	72	3
Grayson and Western (1998)	Tarrawarra, Australia	Grass	Silty loam	1.1E+05 m ²	30	500	13
	Tarrawarra, Australia	Grass	Silty loam	1.1E+05 m ²	60	20	13
	R-5 Chickasha	Grass	Silty loam	1.0E+05 m ²	120	34	84
	Lockyersleigh	/	/	1.0E+09 m	50	41	85
Gómez-Plaza et al.(2000)	Murcia region, Spain	Grass	Lithic Leptosols (FAO)	300 m	15	16	14
				310 m		16	
				200 m		11	
Van Pelt and Wierenga (2001)	Leyendecker NM	Wheat/cotton	Silty clay loam	1.0 E+04 m ²	15-50	60	14
Cosh et al.(2004)	Walnut Creek Iowa	Corn	Silt loam	1.0 E+11 m ²	5	12	43
Bosch et al.(2006)	Georgia (SMEX03)	Forest \cropland \pasture	Loamy sand	3.8 E+09 m ²	6	19	10
Cosh et al.(2008)	Walnut Gulch, Arizona	Rangeland cropland	/	1.5 E+08 m ²	5	21	/
Schneider et al.(2008)	Inner Mongolia, China	Grass	Sandy loam	3.6E+09 m ²	6	400	/
Brocca et al.(2009)	Ponte della Pietra, Italy	Grass	Silty clay	4.05E+03 m ²	10	45	14
	Ingeneria, Italy	Grass	Silty clay loam	5.0E+03 m ²	10	50	14
	Colorso, Italy	Grass (pasture)	Sandy loam	8.8E+03 m ²	10	108	7
Hu et al.(2009)	Liudaogou, China	Grass/shrub/wood/fallow	Sandy loam	2.0E+07 m ²	100	12	20
Gao and Shao (2012a)	Liudaogou, China	Grass	Sandy loam	7.0E+03 m ²	300	91	20

the relationship between SWS temporal stability and soil depth; (2) to assess the effects of land use on profile characteristics of SWS temporal stability; (3) to estimate the mean SWS of the two land uses based on the identifying representative locations of each soil layer.

Material and methods

Study site description

The study was carried out in Liudaogou watershed located in the north of Loess Plateau of China, latitude $35^{\circ}20'–40^{\circ}10' N$ and longitude $110^{\circ}21'–110^{\circ}23' E$. Detailed information about the area can be found in She et al. (2010). The watershed lies at an altitude between 1,081 and 1,274 m and has an area of 6.89 km². The climate is semi-arid with a mean annual rainfall of 437 mm (minimum of 109 mm, maximum of 891 mm) and a mean temperature of 8.4 °C (the minimum temperature is $-9.7^{\circ} C$ in January, and the maximum is $23.7^{\circ} C$ in July). The annual potential evapotranspiration is 785.4 mm, with a desiccation degree of 1.8 and 135 frost-free days. The groundwater table is lower than 20 m beneath soil surface.

Loessal mein soil (Los–Orthic Entisol, Chinese Taxonomic System; Gong 1999) is the predominant soil in the watershed. Sand, loamy sand, and sandy loam are the dominant soil texture classes, the proportions of which to the entire region are 13, 17, and 70 %, respectively. Most of the natural vegetation has been destroyed in the watershed due to long-term human activity and serious wind–water erosion. The watershed is covered by the dominant artificial vegetation, such as *Medicago sativa* L. (grass), and *Caragana korshinskii* (shrub), which accounts for 25 and 9 % of the watershed area, respectively.

Experimental design

Two land uses, each containing eight sampling locations, were selected to pass through *C. korshinskii* (shrub land use, marked from S1 to S8), and *M. sativa* L. (grassland use, marked from G1 to G8) of the watershed (Fig. 1). Each location covers about 500-cm \times 2,000-cm area, and was fenced with iron sheet to prevent human activity. Three aluminum neutron probe access tubes were installed at each location to reach the 400 cm depth. From May 26, 2007 to October 11, 2008, slow neutron accountings were obtained at 19 dates. For each access tube, the neutron counting rate (CR) was measured in 10 cm interval for 0–100 cm, and in interval of 20 cm for 100–400 cm. Volumetric soil water contents, θ (%), at each depth, were calculated for CR using the following calibration curves:

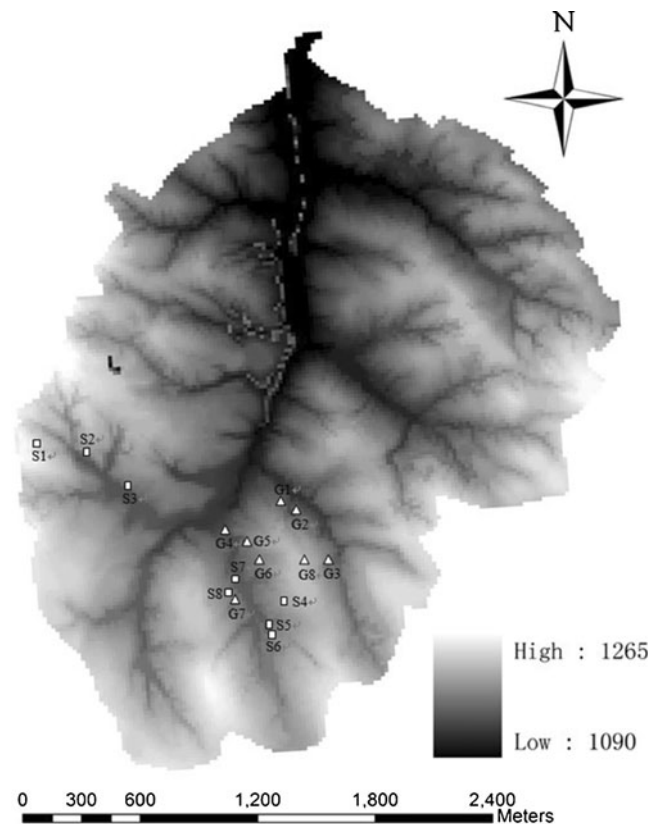


Fig. 1 Distribution of sampling locations (sampling locations are shown by marks that are consecutively numbered; S, G refer to shrub land and grassland use, respectively)

$$\theta = 0.5993 \times CR - 0.0063 (R^2 = 0.75, p < 0.001) \quad (1)$$

For 0–10 cm layer

$$\theta = 0.4857 \times CR - 0.008 (R^2 = 0.75, p < 0.001) \quad (2)$$

For 10–20 cm layer

$$\theta = 0.5723 \times CR - 0.0117 (R^2 = 0.91, p < 0.001) \quad (3)$$

For 20–400 cm layer

The average θ of the three access tubes was used to calculate the SWS for each location. To evaluate the vertical distribution along the profile, soil water storage (in millimeter) of location i at time j in every 40 cm depth were calculated from $\theta(i, j, k)$ (% v/v) data (k refers to different soil depths, in centimeter) by the following equation.

$$\begin{aligned} \text{SWS}_{j(0-40 \text{ cm})}(i) &= \theta(i, j, 10) \times 100 + \theta(i, j, 20) \\ &\quad \times 100 + \theta(i, j, 30) \times 100 \\ &\quad + \theta(i, j, 40) \times 100 \end{aligned} \quad (4)$$

$$\begin{aligned}
 \text{SWS}_{j(40-80 \text{ cm})}(i) &= \theta(i, j, 50) \times 100 + \theta(i, j, 60) \\
 &\quad \times 100 + \theta(i, j, 70) \times 100 \\
 &\quad + \theta(i, j, 80) \times 100 \tag{5}
 \end{aligned}$$

$$\begin{aligned}
 \text{SWS}_{j(80-120 \text{ cm})}(i) &= \theta(i, j, 90) \times 100 + \theta(i, j, 100) \\
 &\quad \times 100 + \theta(i, j, 120) \times 200 \tag{6}
 \end{aligned}$$

$$\begin{aligned}
 \text{SWS}_{j(120-160 \text{ cm})}(i) &= \theta(i, j, 140) \times 200 + \theta(i, j, 160) \times 200 \dots \dots \tag{7}
 \end{aligned}$$

$$\begin{aligned}
 \text{SWS}_{j(360-400 \text{ cm})}(i) &= \theta(i, j, 380) \times 200 + \theta(i, j, 400) \\
 &\quad \times 200 \tag{8}
 \end{aligned}$$

At each location, a 100 cm deep pit was excavated to take undisturbed soil samples. Soil bulk density and saturated soil water content were determined by the gravimetric method. The field capacity and permanent wilting point were determined with a pressure plate apparatus (Cassel and Nielsen 1986) at -33 and -1,500 kPa, respectively.

Methods of statistical analysis

According to Vachaud et al. (1985), two statistical techniques were used for temporal stability analysis:

- (1) Spearman non-parametric test (r_s). This index was used to characterize the persistence of SWS spatial pattern with time (Vachaud et al. 1985; Brocca et al. 2009), defined by:

$$r_s = 1 - \frac{6 \sum_{i=1}^n (R_{ij} - R_{ij'})^2}{n(n^2 - 1)} \tag{9}$$

where R_{ij} is the rank of SWS at location i at time j and $R_{ij'}$ is the rank of SWS observation at the same location, but at time j' . n is the number of sampling locations.

- (2) Parametric test of relative difference. The relative difference, δ_{ij} , is defined as (Vachaud et al. 1985):

$$\delta_{ij} = \frac{\Delta_{ij}}{\overline{\text{SWS}}_j} \tag{10}$$

where

$$\Delta_{ij} = \text{SWS}_{ij} - \overline{\text{SWS}}_j \tag{11}$$

and

$$\overline{\text{SWS}}_j = \frac{1}{n} \sum_{i=1}^n \text{SWS}_{ij} \tag{12}$$

SWS_{ij} being the soil water storage at location i at time j . Thus, for each location i , the mean relative difference (MRD) $\bar{\delta}_i$ and its standard deviation (SDRD) $\sigma(\delta_i)$ are given by:

$$\bar{\delta}_i = \frac{1}{m} \sum_{j=1}^m \delta_{ij} \tag{13}$$

$$\sigma(\delta_i) = \sum_{j=1}^m \left(\frac{\delta_{ij} - \bar{\delta}_i}{m - 1} \right)^{1/2} \tag{14}$$

where m is the number of sampling dates. Obviously, a “stable” location in time is characterized by a low value of SDRD.

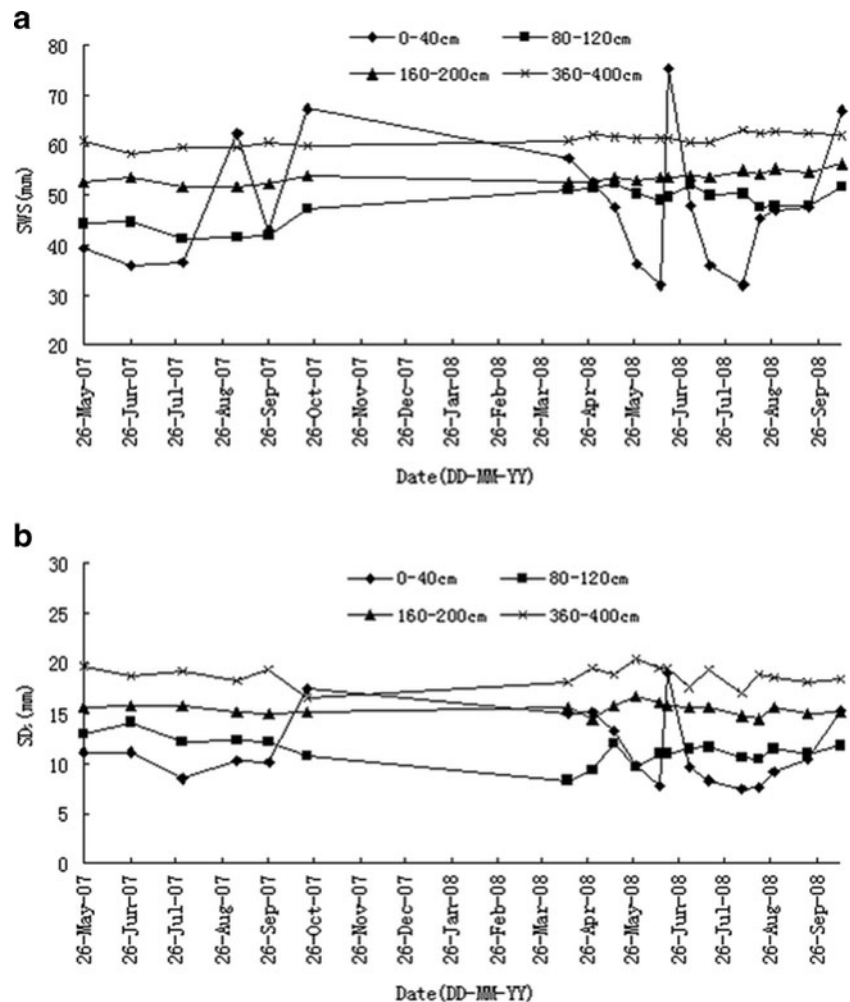
Results and Discussion

Temporal-spatial analysis of profile SWS

Four soil layers (0–40, 80–120, 160–200, and 360–400 cm) were selected for graphing analysis of the time series of mean SWS over space and their corresponding standard deviation (SD_s) (Figs. 2 and 3). For the two land uses, time changes of SWS were mainly observed for the shallow soil layers. In the grass and shrub land uses, spatial mean SWS of 0–40 cm soil layer ranged from 31.9 to 75.2 mm and from 20.8 to 67.2 mm during the study period, with time-averaged mean SWS being 47.8 and 37.8 mm, respectively. Compared to the saturated SWS (204 mm), field capacity (120 mm) and permanent wilting point SWS (22.4 mm) for the 0–40 cm soil layer, the measured low SWS was a critical factor for vegetation restoration in this area. The temporal changes of SWS gradually decreased for deeper soil layers. Ranges of spatial averaged SWS were 11.1, 4.5, and 4.7 mm for the three deeper soil depths (80–120, 160–200, 360–400 cm), respectively, in the grassland use (Fig.2a) and 16.4, 4.6, and 3.6 mm respectively, in the shrub land use (Fig.3a).

Spatial variability of SWS, as indicated by SD_s , followed a trend that was positively correlated with mean SWS, with Pearson correlation coefficient of 0.693 ($p < 0.01$) for the grassland use and 0.461 ($p < 0.05$) for the shrub land use. This indicates stronger spatial variability of SWS under wetter conditions, which could partly be explained by the actively vertical and lateral redistribution of soil moisture following significant storm events (Famiglietti et al. 1998).

Fig. 2 Time series of **a** the mean soil water storage (SWS) over space, **b** its associated standard deviation (SD_s) for various soil layers of grassland

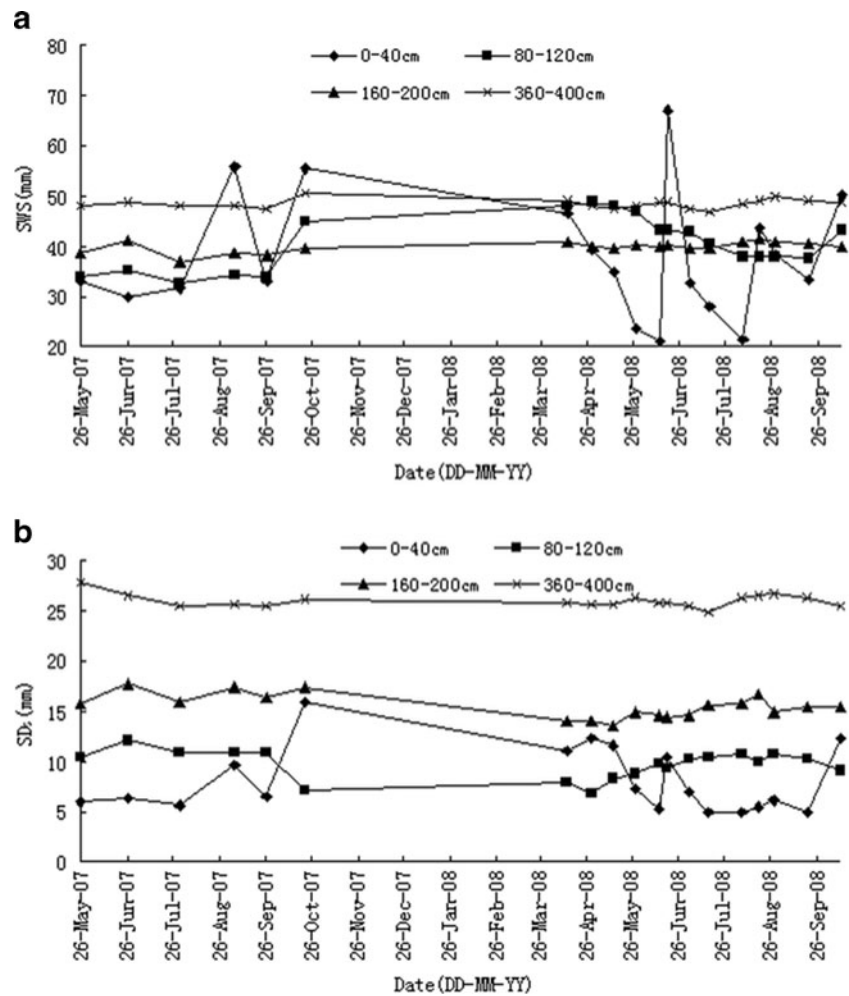


Compared to dry conditions, soil moisture variability under wet condition is likely controlled more by variations in hydraulic conductivity, leading to more SWS variations. The positive correlation of soil water condition and associated variability were also observed by other researchers (Famiglietti et al. 1998; Hu et al. 2009). Similar to the mean SWS, the SD_s changed more over time for the shallow soil layers than for the deep layers (Figs. 2b and 3b).

Typical dry (30-Jul-07) and wet conditions (16-Jun-08), and time-averaged SWS were selected to draw detailed profile characteristics of SWS and corresponding statistical parameters (Figs. 4 and 5). Time averaged SWS showed an increasing trend with soil depth, with SWS values increasing from 47.8 mm to 61.2 mm for the grassland and from 37.8 to 48.5 mm for the shrub land. The increasing trend of soil moisture with depth was also observed in other places on the Chinese Loess Plateau (Qiu et al. 2001). Results of ANOVA test revealed significant differences for SWS between shallow soil layers and deeper soil depths, and between the two land uses ($p < 0.05$). Combinations of factors

including rainfall, infiltration, upward water movement, and water uptake by plant roots affect SWS. In the study region, shrub land (*C. korshinskii*) could produce a denser root system, larger leaf canopy, and thus more ET and lower SWS than that in the grassland (*M. sativa* L.) use. A comparison of the SWS pattern between the dry and wet conditions revealed that the profile changes of SWS during the study period occurred down to 280 cm depth in the shrub land, but only down to 160 cm in the grassland (Fig. 4). The SWS at 0–40 cm was 31.7 mm on 30-Jul-07 (dry), and increased to 67.2 mm on 16-Jun-08 (wet) for the shrub land; and 36.6 mm on the dry day, then increased to 75.2 mm on the wet day for the grassland. These increasing ranges were gradually reduced with the increase of soil depth. The profile SWS curves deeper than 280 cm for the shrub land on the two typical days were almost superposed compared to 160 cm for the grassland. Profile characteristics of SD_s further proved that SWS of deeper soil layers had greater spatial variability, which was significant ($p < 0.05$) by a one-way ANOVA test.

Fig. 3 Time series of **a** the mean soil water storage (SWS) over space, **b** its associated standard deviation (SD_S) for various soil layers of shrub land



The time-averaged SD_S values for the soil layers with increasing depth ranged from 10.9 to 18.7 mm for the grassland, and from 8.1 to 26.0 mm for the shrub land, respectively (Fig. 4).

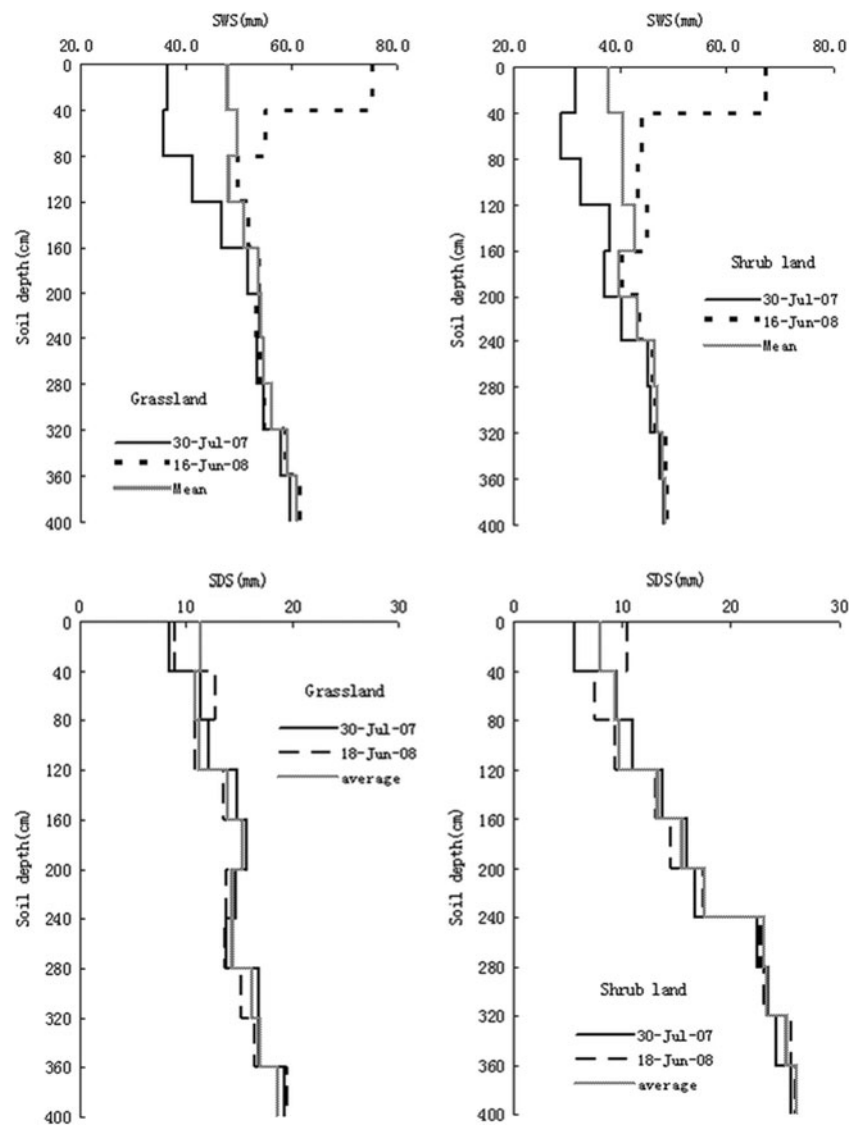
Profile distribution of the standard deviation and coefficient of variation over time (SD_T and CV_T) showed an inverse trend compared to SWS and SD_S , which indicated that temporal changes for the SWS decreased with increasing soil depth (Fig. 5). Additionally, this decrease was mainly observed in the upper soil layers, especially at the depth of 0–200 cm. The values of SD_T and CV_T for 0–40 cm depth were 12.8 mm and 26.8 % in the grassland use, and 12.5 mm and 33.1 % in the shrub land use. They decreased sharply to 1.2 mm and 2.3 % in the grassland, and 1.1 mm and 2.9 % in the shrub land use at the layer of 160–200 cm, respectively. SD_T and CV_T below the 200 cm soil depth remained consistently low, at about 1.0 mm and 1.8 %, with minor changes for both land uses. Higher temporal variability of SWS of shallow soil layers may be related to the some environmental factors, including rainfall, surface evaporation, and water uptake by plant roots. These results are consistent with previous observations (Choi and Jacobs

2007; Gao and Shao 2012a), but varied with change in depth at different study areas.

Profile characteristics of temporal patterns of SWS

The matrix of the r_s made from pairs of SWS measured at the 8 sites for all 19 dates showed that all coefficients were significant at the 0.01 probability level (data not shown owing to the large amount of space that it would occupy) and statistical test indicated a strong temporal stability of spatial patterns for all soil layers (Fig. 6). The results were consistent with the findings of Vachaud et al.(1985) and Tallon and Si (2004). Mean values of r_s were 0.93 and 0.94 for the shrub land and grassland uses, respectively, which were comparable to those of Hu et al. (2009), and larger than those of Brocca et al. (2009). The profile curves of the mean r_s presented increasing trends with soil depth, and the increasing trend of mean r_s mainly occurred at the depth of 0–200 cm. For soil layers below 200 cm, mean r_s maintained the high level for both land uses. The increased time stability with soil depth was consistent with most findings for various land use conditions in a variety of

Fig. 4 Profile characteristics of the soil water storage (SWS) over space and its associated standard deviation (SD_S) on typical dry condition (30-Jul-07), wet condition (18-Jun-08) and time average over all measurement for the grassland and shrub land uses



places and over a large range of time–space scales (Cassel et al. 2000; Lin 2006; Guber et al. 2008). The higher root water uptake (Hupet and Vanclooster 2002) and more meteorological effect (Hu et al. 2010a) may be the main reason for weaker time stability at shallow depth. Deeper depths are immune to those effects, and thus have an increased time stability (Kamgar et al. 1993).

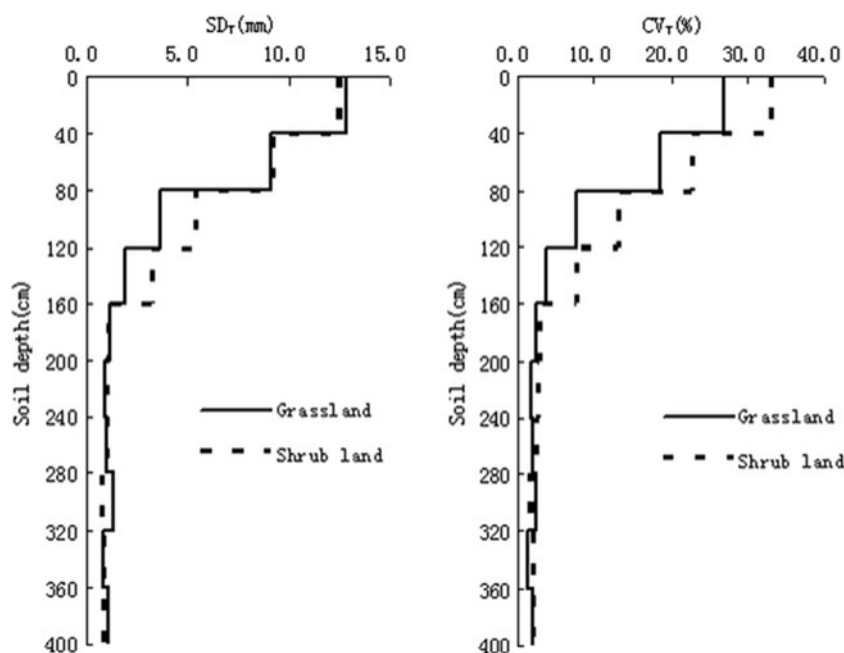
Temporal stability analysis of profile SWS

Figure 7 presents the rank ordered MRD and associated SDRD of SWS in diverse soil layers for the two land uses. The two variables behaved differently at various soil depths (Fig. 8).

The mean ranges of MRD at soil depth of 0–40 cm were 62.5 % for the shrub land use, and 55.7 % for the grassland use, and then increased to 130.5 and 88.0 %, respectively, at soil layer of 360–400 cm. The increasing trend of ranges of

MRD corresponded with the increasing spatial variability of SWS with soil depth, as indicated by the SD_S values (Fig. 4), although there were some fluctuations in the middle of the profile. The ranges of MRD for the both land uses were lower than other published results. For example, Hu et al. (2010a) reported that the ranges of MRD were greater than 180 % for all soil depths within the 0.8 m soil depth. This could be attributed to the more diverse and complex nature in relation to soil, topographic and vegetation properties in their study area (Hu et al. 2010b). The effect of land use on MRD is evident, and which was also dependent on soil depth. For 0–200 cm, the ascending order curves of MRD for the two land uses were almost superposed. However, below 200 cm soil depth, the representative dry locations in the shrub land use had lower MRD values and the wet locations had larger values than that in the grassland use. These differences became more obvious with increasing soil depth, which resulted in significantly larger MRD at

Fig. 5 Profile characteristics of standard deviation of the time series of the mean spatial SWS (SD_T) and the coefficient of variation of the time series of the mean spatial SWS (CV_T) for the grassland and shrub land uses



200–400 cm soil depth for the shrub land use than that for the grassland use ($p < 0.05$). These results also confirmed the higher spatial variability of SWS for deeper soil layers in the shrub land use.

The low SDRD was used as an indicator to describe the temporal stability of SWS. Figure 7 shows that locations having higher MRD values at shallower soil layers had much weaker temporal stability than those at deeper soil depths. The mean SDRD on the shrub land use was 9.3 % at 0–40 cm depth and decreased to 3.5 % with increasing soil

depth to 240–280 cm layer. For the grassland use, the mean SDRD also decreased with soil depth: 9.6, 9.6, 8.1, and 5.2 % for the 0–40, 40–80, 80–120, and 120–160 cm soil depth, respectively. The mean SDRD remained almost the same (about 3 to 4 %) for the soil layers deeper than 280 cm on the shrub land use and deeper than 160 cm on the grassland use.

The relationship between temporal stability and soil depth was illustrated consistently by the profile distribution of mean SD_T and CV_T , which was also reported in an agricultural field (Guber et al. 2008) and a forest ecosystem (Lin 2006). At the same time, the results of temporal stability as indicated by SDRD were consistent with those based on the r_s , although these two indices present different concepts of temporal stability (Hu et al. 2010a; 2012). The r_s described the similarity of the spatial pattern over time, while the SDRD results mainly presented the degree of temporal invariability for a specific location. Therefore, for the study land uses, the profile characteristics of the time-similarity of spatial patterns of SWS showed a concordant trend with the temporal stability of the locations, which was also reported by Gao and Shao (2012a). Hu et al. (2010b), however, got the opposite results of the inconsistency between r_s and SDRD, which were largely due to the different sampling depths.

The increasing temporal stability with depth could mainly explained by the fact that the dependency of soil moisture on climatic, biological and hydrological factors decreases with increasing soil depth (Hupet and Vanclooster 2002; Starks et al. 2006; Gao and Shao 2012a, b). Another explanation was that soil structure and its ability to retain water more variable in shallow soil layers (Korsunskaya et al. 1995). In our study area, the depth of about 280 cm for

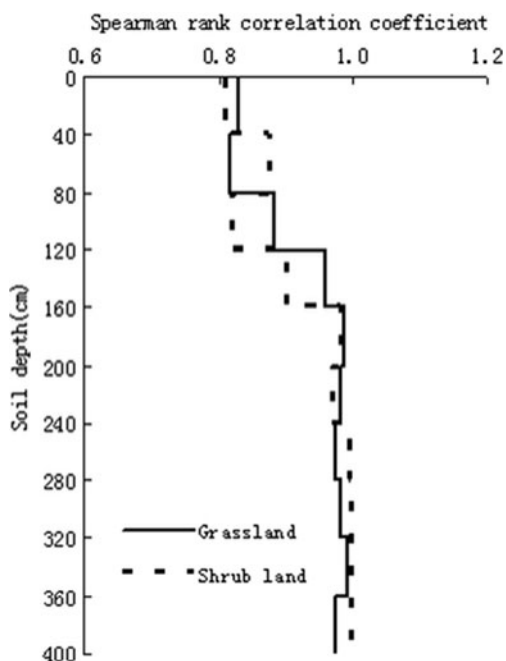
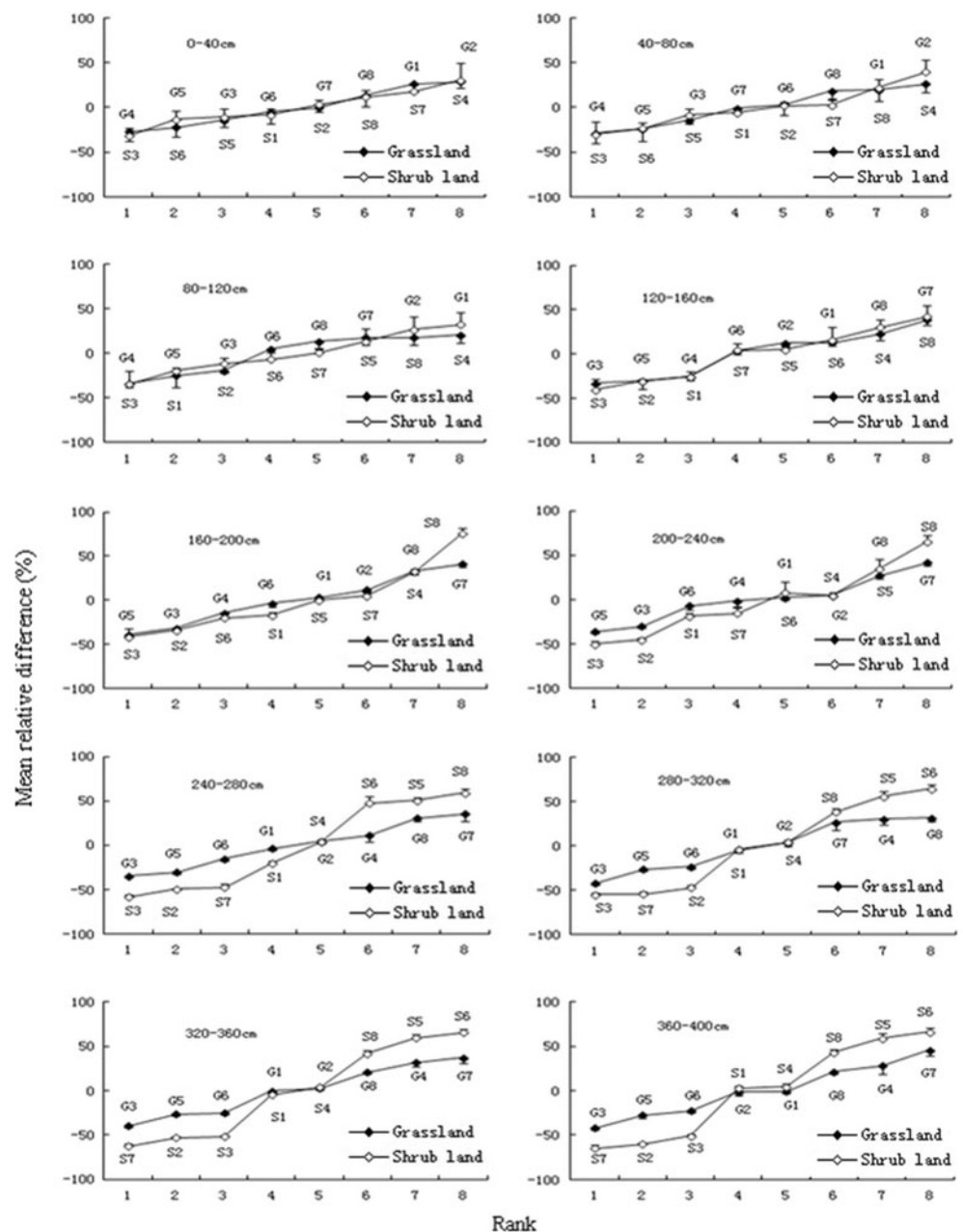


Fig. 6 Profile characteristics of the mean Spearman rank correlation coefficient

Fig 7 Ranked averages of the relative differences of the SWS data at various soil depths for two land use. Bars represent \pm one standard deviation, σ (δ), number refers to the measurement location

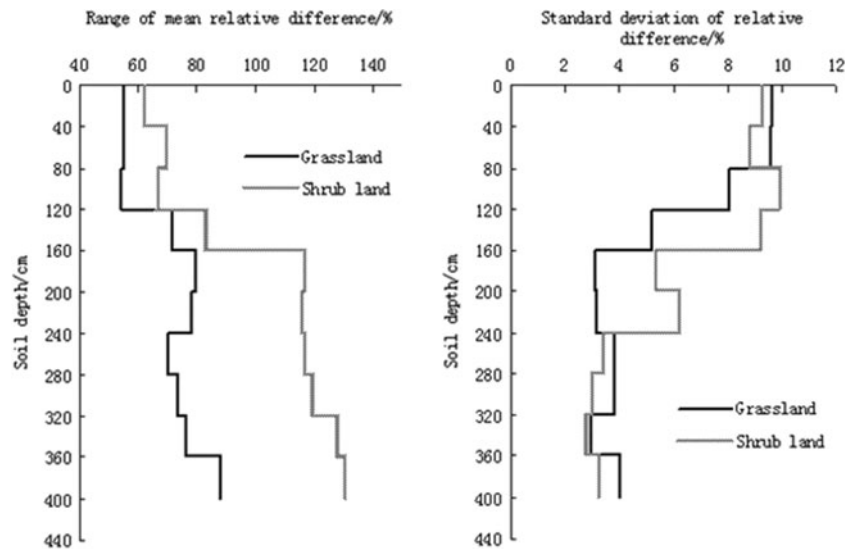


the shrub land use, and 160 cm for the grassland use could be as the boundary between the temporal unstable and stable layer of profile SWS. For deeper than the boundary, the effects of infiltration and evapotranspiration became small and, the input and output terms of water balance almost reached equilibrium at seasonal scales. Considering the high dependence of temporal stability on depth, caution should be taken in making the sampling plan to determine SWS values. Therefore, increasing sampling frequency at shallow soil layers is a reasonable measure for improving the precision of prediction. Furthermore, a significant reduction in number of required samples, while maintain a high level of prediction can be achieved by optimizing representative sites at deep soil layers.

Identification of representative locations based on relative difference analysis

Based on the relative difference method, we could find that some given locations systematically represent the mean SWS of the study land use or give under- or over-estimate of the mean SWS regardless of the observation time. Mathematically, the temporally stable locations to estimate the mean SWS of a study area should have a MRD value that is the closest to zero and, additionally, a low SDRD value (Grayson and Western 1998). The allowable bias from the mean for MRD is 5 % in this study. Then, the number of locations meets the required was just only 2 to 3 for all the soil layers (Fig. 7), which may be due to the strong spatial

Fig. 8 Profile characteristics of the range of mean relative difference and its standard deviation



variability in SWS of the two land use, especially for deeper soil layers.

The lower the value of SDRD, the more temporally stable a location would be. Starks et al. (2006) identified locations as time stable those with SDRD values lower than 5 %. In light of this principle, an increase in depth resulted in a higher number of time-stable locations in the present study. Only one to three locations in a total of eight spatial observations were time stable for the shallow soil layers, especially 0–40, 40–80, and 80–120 cm soil depth. For the deeper soil layers, the SDRD values for majority of the locations were lower than 5 %, which meant that almost overall spatial pattern of deep SWS in the study land uses were temporal stable.

Locations meeting both of the MRD and SDRD requirements could directly represent the mean SWS of the study land uses (Tables 2 and 3). The number of representative locations in both land uses increased with

increasing soil depth. Only one location for the diverse soil layers above the boundary (depths of about 280 cm for the shrub land use, and about 160 cm for the grassland use), could be used to directly predict the mean SWS of the area. The number of representative location increased to two for deeper soil layers. These results agreed with the findings of Gao and Shao (2012a), who indicated that although the large spatial variability of soil moisture resulted in fewer locations with MRD values close to zero, the decreasing temporal variability of soil moisture induced more locations with smaller SDRD values in deeper soil layers. Compared to spatial variability, temporal variability of soil moisture had a more pronounced effect on identifying representative locations, thus an increase in soil depth resulted in more representative locations.

No single location could represent the mean SWS for all ten soil layers (Tables 2 and 3). Especially above the

Table 2 Summary statistics for representative locations for shrub land use, and evaluation of its predictive accuracy according to four criteria

Depth (cm)	Location	Rank	MRD(%)	SDRD(%)	R^2	E	RMSE(%)	MAE(%)
0–40	S2	5	3.51	4.54	0.86	0.83	1.76	0.25
40–80	S2	5	2.33	4.18	0.85	0.59	2.10	0.46
80–120	S7	5	0.67	4.66	0.94	0.71	1.89	0.34
120–160	S5	5	4.85	4.70	0.96	0.78	1.95	0.29
160–200	S5	5	0.03	3.68	0.73	0.42	2.25	0.15
200–240	S4	6	4.52	2.67	0.92	0.89	1.36	0.28
240–280	S4	5	3.35	2.79	0.89	0.86	1.21	0.16
280–320	S1	4	–3.71	1.52	0.91	0.93	1.34	0.11
	S4	5	4.59	2.57	0.95	0.89	1.05	0.08
320–360	S1	4	–4.38	2.23	0.96	0.97	1.12	0.13
	S4	5	3.80	1.93	0.89	0.95	1.09	0.04
360–400	S1	4	2.99	2.73	0.93	0.92	1.01	0.08
	S4	5	4.80	2.96	0.91	0.97	1.13	0.12

MRD mean relative difference, SDRD standard deviation of relative difference, R^2 coefficient of determination, E Nash–Sutcliffe coefficient, RMSE root mean square error, MAE mean absolute error

Table 3 Summary statistics for representative locations for grassland use, and evaluation of its predictive accuracy according to four criteria

Depth (cm)	Location	Rank	MRD(%)	SDRD(%)	R^2	E	RMSE(%)	MAE(%)
0–40	G7	5	−0.22	4.98	0.90	0.78	1.86	0.25
40–80	G7	4	−1.12	4.01	0.83	0.62	2.12	0.34
80–120	G6	4	4.84	4.04	0.88	0.72	1.94	0.45
120–160	G6	4	3.87	4.34	0.91	0.89	1.56	0.26
160–200	G1	5	3.14	2.01	0.92	0.79	1.98	0.13
200–240	G1	5	1.80	2.71	0.98	0.92	1.36	0.09
	G2	6	4.32	2.02	0.95	0.91	1.48	0.19
240–280	G1	4	−3.60	2.68	0.91	0.86	1.26	0.20
	G2	5	4.43	2.38	0.87	0.93	1.10	0.16
280–320	G1	4	−4.13	2.90	0.93	0.94	1.26	0.09
	G2	5	3.53	3.33	0.97	0.97	1.13	0.11
320–360	G1	4	−0.57	2.24	0.92	0.94	1.08	0.15
	G2	5	2.63	2.66	0.89	0.89	1.20	0.06
360–400	G1	4	−1.54	3.76	0.96	0.95	1.05	0.14
	G2	5	−1.06	2.22	0.91	0.96	1.11	0.10

MRD mean relative difference, *SDRD* standard deviation of relative difference, R^2 coefficient of determination, E Nash–Sutcliffe coefficient, *RMSE* root mean square error, *MAE* mean absolute error

boundary depth, most of the representative locations were different at different soil depths, which Guber et al. (2008) also reported. But, for layers deeper than the boundary, some of our locations could represent the mean SWS for all layers. For example, locations S1 and S4 could be used to monitor the mean value at the 280 to 400 cm soil depths in the shrub land use, and locations G1 and G2 could be used to monitor the mean value at the 160 to 400 cm soil depth in the grassland use. This similar ranking of the locations for deep soil layers could be explained by the weak variability in soil texture properties of deep loess profile (Wang et al. 2010). Zhao et al. (2010) also pointed out that the temporal patterns of soil moisture are significantly affected by vertical variability of soil properties, especially the soil texture. For the shallow soil layers, the soil variability along soil profile is introduced with the activity of soil organisms, soil erosion, and the growth of the vegetation (Gao and Shao 2012b). The combined effects of soil, vegetation, and topographic properties determined the differences in the representative locations at different soil layers above boundary depth.

The accuracy of prediction for the representative locations was further examined using the independent dataset measured in 2006 as a validation dataset. The different performance evaluation criterion used to find the applicability and comparison of representative locations in diverse soil layers are correlation coefficient (R^2), Nash–Sutcliffe coefficient (E), root mean square error (RMSE) and mean absolute error (MAE). The formula to calculate these performance evaluation criteria are given by Jyoti et al. (2012). The high R^2 values combined with linear gradients having values of 0.73 to 0.98, indicating that the selected

representative locations would provide good estimates of mean SWS. Nash–Sutcliffe coefficient (E) represents the initial uncertainty explained by the representative locations. The closer the value to 1, the better is the representative location performance. For both land uses, the E values presented increasing trends with increasing soil depth, which ranged from 0.42 to 0.97 in the shrub land use, and from 0.62 to 0.97 in the grassland use. RMSE and MAE values also showed decreasing trends with increasing soil depth in both land uses, which further proved that stronger temporal stability of SWS in deeper soil layers. The predictive accuracies were comparable to those reported by Brocca et al. (2009). The predictions were reliable based on Cosh et al. (2008), who stated that an estimate was accurate when RMSE was less than 2 %.

Conclusions

In the present work, temporal behavior of profile SWS has been investigated in two land uses (grassland and shrub land) in the Chinese semi-arid region. With increasing soil depth, temporal variability of SWS decreased, while its spatial variability increased. Greater temporal stability was observed at deeper soil layers, based on either the Spearman rank correlation coefficient (r_s) or the SDRD index. The boundary between the temporally unstable and stable layer of profile SWS happened at 280 cm depth in the shrub land use and 160 cm depths for the grassland use. No single location could represent the mean SWS for all ten soil layers. Especially above the boundary depth, only one different location for each soil layers could be used to directly predict the mean SWS of the area. But for temporal

stable layers, more and same locations estimated the mean SWS of the study land uses accurately. Locations S1 and S4 could be used to monitor the mean value at the 280 to 400 cm soil depths in the shrub land use, and locations G1 and G2 could be used to monitor the mean value at the 160 to 400 cm soil depth in the grassland use. The accuracy of prediction for the representative locations also increased with increasing soil depth. These findings provide useful guidance for future research work related to planning of soil sampling and soil water management in semi-arid region.

Acknowledgment We acknowledge the financial support provided by National Nature Science Foundation of China through grants No. 51109063, the Open Funding Project (Y152741s04) of the Key Laboratory of Aquatic Botany and Watershed Ecology, Chinese Academy of Sciences, and China Postdoctoral Science Foundation (2011 M500115, 2012 T50433).

References

- Bosch DD, Lakshmi V, Jackson TJ, Choi M, Jacobs JM (2006) Large scale measurements of soil moisture for validation of remotely sensed data: Georgia soil moisture experiment of 2003. *J Hydrol* 323:120–147
- Brocca L, Melone F, Moramarco T, Morbidelli R (2009) Soil moisture temporal stability over experimental areas in Central Italy. *Geoderma* 148:364–374
- Cassel DK, Nielsen DR (1986) Field capacity and available water capacity. In: Klute, A.(Ed.), *Methods of Soil Analysis*. Part 1, second ed. Agron Monogr 9 ASA and SSSA, Madison, WI, pp: 901–926
- Cassel DK, Wendroth O, Nielsen DR (2000) Assessing spatial variability in an agricultural experiment station field: opportunities arising from spatial dependence. *Agron J* 92:706–714
- Choi M, Jacobs JM (2007) Soil moisture variability of root zone profiles within SMEX02 remote sensing footprints. *Adv Water Resour* 30:883–896
- Cosh MH, Jackson TJ, Bindlish R, Prueger JH (2004) Watershed scale temporal and spatial stability of soil moisture and its role in validating satellite estimates. *Remote Sens Environ* 92:427–435
- Cosh MH, Jackson TJ, Moran S, Bindlish R (2008) Temporal persistence and stability of surface soil moisture in a semi-arid watershed. *Remote Sens Environ* 112:304–313
- da Sivaró AP, Nadler AN, Kay BD (2001) Factors contributing to temporal stability in spatial patterns of water content in the tillage zone. *Soil Tillage Res* 58:207–218
- Famiglietti JS, Rudnicki JW, Rodell M (1998) Variability in surface moisture content along a hillslope transect: Rattlesnake Hill, Texas. *J Hydrol* 210:259–281
- Gao L, Shao MA (2012a) Temporal stability of soil water storage in diverse soil layers. *Catena* 95:24–32
- Gao L, Shao MA (2012b) Temporal stability of shallow soil water content for three adjacent transects on a hillslope. *Agr Water Manage* 110:41–54
- Gómez-Plaza A, Alvarez-Rogel J, Albaladejo J, Castillo VM (2000) Spatial patterns and temporal stability of soil moisture across a range of scales in a semi-arid environment. *Hydrol Process* 14:1261–1277
- Gong ZT (1999) *Chinese soil taxonomy: theory, method, practice*. Science, Beijing, pp 23–28
- Grant L, Seyfried M, McNamara J (2004) Spatial variation and temporal stability of soil water in a snow-dominated, mountain catchment. *Hydrol Process* 18:3493–3511
- Grayson RB, Western AW (1998) Towards areal estimation of soil water content from point measurements: time and space stability of mean response. *J Hydrol* 207:68–82
- Guber AK, Gish TJ, Pachepsky YA, van Genuchten MT, Daughtry CST, Nicholson TJ, Cady RE (2008) Temporal stability in soil water content patterns across agricultural fields. *Catena* 73:125–133
- Heathman GC, Larose M, Cosh MH, Bindlish R (2009) Surface and profile soil water spatio-temporal analysis during an excessive rainfall period in the Southern Great Plains, USA. *Catena* 78:159–169
- Hu W, Shao MA, Han FP, Reichardt K, Tan J (2010a) Watershed scale temporal stability of soil water content. *Geoderma* 158:181–198
- Hu W, Shao MA, Reichardt K (2010b) Using a new criterion to identify sites for mean soil water storage evaluation. *Soil Sci Soc Am J* 74:762–773
- Hu W, Shao MA, Wang QJ, Reichardt K (2009) Time stability of soil water storage measured by neutron probe and the effects of calibration procedures in a small watershed. *Catena* 79:72–82
- Hu W, Tallon LK, Si BC (2012) Evaluation of time stability indices for soil water storage upscaling. *J Hydrol* 475:229–241
- Hupet F, Vanclooster M (2002) Intraseasonal dynamics of soil moisture variability within a small agricultural maize cropped field. *J Hydrol* 261:86–101
- Ibrahim HM, Huggins DR (2011) Spatio-temporal patterns of soil water storage under dryland agriculture at the watershed scale. *J Hydrol* 404:186–197
- Jyoti PS, Paramartha D, Arindrajit P (2012) Delay prediction in mobile Ad Hoc net work using artificial neural network. *Procedia Technol* 4:201–206
- Kachanoski RG, de Jong E (1988) Scale dependence and the temporal persistence of spatial patterns of soil water storage. *Water Resour Res* 24:85–91
- Kamgar A, Hopmans JW, Wallender WW, Wendroth O (1993) Plot size and sample number for neutron probe measurements in small field trials. *Soil Sci* 156:213–224
- Korsunskaya LP, Gummatov NG, Pachepsky YA (1995) Seasonal changes in root biomass carbohydrate content, and structural characteristics of Gray Forest soil. *Eurasian Soil Sci* 27:45–52
- Lin H (2006) Temporal stability of soil moisture spatial pattern and subsurface preferential flow pathways in the Shale Hills catchment. *Vadose Zone J* 5:317–340
- Martínez-Fernández J, Ceballos A (2003) Temporal stability of soil moisture in a large-field experiment in Spain. *Soil Sci Soc Am J* 67:1647–1656
- Penna D, Brocca L, Borga M, Dalla Fontana G (2013) Soil moisture temporal stability at different depths on two alpine hillslopes during wet and dry periods. *J Hydrol* 477:55–71
- Qiu Y, Fu BJ, Wang J, Chen LD (2001) Soil moisture variation in relation to topography and land use in a hillslope catchment of the Loess Plateau, China. *J Hydrol* 240:243–263
- Schneider K, Huisman JA, Breuer L, Zhao Y, Frede HG (2008) Temporal stability of soil moisture in various semi-arid steppe ecosystems and its application in remote sensing. *J Hydrol* 359:16–29
- She DL, Liu YY, Shao MA, Timm LC, Yu SE (2012) Temporal stability of soil water content for a shallow and deep soil profile at a small catchment scale. *Aust J Crop Sci* 6(7):1192–1198
- She DL, Shao MA, Timm LC, Pla Senti I, Reichardt K, Yu SE (2010) Impacts of land use pattern on soil water content variability in the Loess Plateau of China. *Acta Agric Scand Sect B Soil Plant Sci* 60:369–380

- Starks PJ, Heathman GC, Jackson TJ, Cosh MH (2006) Temporal stability of soil moisture profile. *J Hydrol* 324:400–411
- Tallon LK, Si BC (2004) Representative soil water benchmarking for environmental monitoring. *J Environ Inform* 4:28–36
- Thierfelder TK, Grayson RB, von Rosen D, Western AW (2003) Inferring the location of catchment characteristic soil moisture monitoring sites. Covariance structures in the temporal domain. *J Hydrol* 280:13–32
- Vachaud G, Passerat De Silans A, Balabanis P, Vauclin M (1985) Temporal stability of spatially measured soil water probability density function. *Soil Sci Soc Am J* 49:822–828
- Van Pelt RS, Wierenga PJ (2001) Temporal stability of spatially measured soil matric potential probability density function. *Soil Sci Soc Am J* 65:668–677
- Vanderlinden K, Vereecken H, Hardelauf H, Herbs M, Martínez G, Cosh MH, Pachepsky YA (2012) Temporal stability of soil water contents: a review of data and analyses. *Vadose Zone J*. doi:10.2136/vzj2011.0178
- Vivoni ER, Gebremichael M, Watts CJ, Bindlish R, Jackson TJ (2008) Comparison of ground-based and remotely-sensed surface soil moisture estimates over complex terrain during SMEX04. *Remote Sens Environ* 112:314–325
- Wang YQ, Shao MA, Shao HB (2010) A preliminary investigation of the dynamic characteristics of dried soil layers on the Loess Plateau of China. *J Hydrol* 381:9–17
- Williams CJ, McNamara JP, Chandler DG (2009) Controls on the temporal and spatial variability of soil moisture in a mountainous landscape: the signature of snow and complex terrain. *Hydrol Earth Syst Sci* 13:1325–1336
- Zhao Y, Peth S, Wang XY, Lin H, Horn R (2010) Controls of surface soil moisture spatial patterns and their temporal stability in a semi-arid steppe. *Hydrol Process* 24:2507–2519